Effect of cathode material on electro-Fenton process efficiency for electrocatalytic mineralization of the antibiotic sulfamethazine

Flamur Sopaj, Nihal Oturan, Jean Pinson, Fetah I. Podvorica, Mehmet A. Oturan

Effect of Cathode Material on Electro-Fenton Process Efficiency for Electrocatalytic Mineralization of the Antibiotic Sulfamethazine

Flamur Sopaj[a,b], Nihal Oturan[a], Jean Pinson[c], Fetah I. Podvorica[b], Mehmet A. Oturan[a,*]

[a] *Université Paris-Est, Laboratoire Géomatériaux et Environnement (EA 4508), UPEM, 5 Bd Descartes, 77454 Marne-la-Vallée, Cedex 2, France.*

[b] *Chemistry Department of Natural Sciences Faculty, University of Prishtina, rr. "Nëna Tereze" nr. 5, 10 000 Prishtina, Kosovo*

[c] *Université de Paris, ITODYS, CNRS, UMR 7086, 15 rue J-A de Baïf, F-75013 Paris, France*

* **Correspondence to:**

Mehmet A. Oturan: mehmet.oturan@univ-paris-est.fr

Abstract

Cathode material plays a crucial role in electro-Fenton process since its efficiency depends to the ability of the cathode material to generate H_2O_2 which control the production rate of hydroxyl radicals, the main oxidizing agent for destruction of organic pollutants. Therefore, this study focused on the role of different cathode materials (i.e., carbon sponge (CS) of five different porosities, carbon felt (CF), and stainless steel (SS)) on the electrochemical oxidation and mineralization of sulfamethazine (SMT) in aqueous solution. Prior to studying the degradation and mineralization power of the cathodes under examination, we performed a systematic study of the production of H_2O_2. It was found that all the carbon sponge cathodes give the high amounts of H_2O_2 in the solution, the most effective being the 45 ppi (pore per linear inch) porosity followed by carbon felt cathode. Stainless steel only gives poor amounts of H_2O_2 for current of 50 and 100 mA. The degradation and mineralization experiments were consistent with the yield of H_2O_2 for all electrolytic systems; electrolytic cells with higher H_2O_2 production capacity showed better performance on SMT degradation/mineralization. The most effective electrolytic system for SMT removal from polluted water was Pt/CS 45 ppi reaching a mineralize rate of 91.1% at 300 mA while the less effective was Pt/SS with only 41% mineralization.

Keywords: Electro-Fenton; Carbon felt; Carbon sponge, Sulfamethazine; Mineralization

Introduction

Large amount of micropollutants (pesticides, dyes, biocides, pharmaceuticals and care products…) issued from different chemical industry activities are continuously discharged to the natural water bodies resulting in their accumulation due to their bio-refractory character. Nowadays, they are detected in natural water streams, even frequently in drinking water sources. The presence of these organic micropollutants and their environmental degradation products in water bodies represents a growing concern over the world [1-8]. These compounds are frequently toxic to water organisms as well as to humans leading, therefore to the intensification of research on new and clean water treatment techniques. The conventional water treatment methods developed so far do not provide total and permanent removal of organic micropollutants from water as they simply separate the organic contaminants [9,10] leading to the formation of concentrated waste (to be further displayed or incinerated) or to eliminate only the biodegradable fraction of organics [11].

On the other hand, effective water treatment technologies, so called advanced oxidation processes (AOPs), were developed during the last decades [12-18]. Based on in situ generation of strong oxidants such as hydroxyl radical ($^{\bullet}OH$) with very high oxidation power (E° = 2.8 V/SHE) and high reactivity, AOPs are able to oxidize organic micropollutants until their ultimate oxidation degree, i.e., mineralization [19-21]. Among the AOPs, the best known is the Fenton process which relies on the reaction using Fenton's reagent (a mixture of H_2O_2 and ferrous iron) to produce $^{\bullet}OH$ according to the following reaction (Eq. (1)):

$$H_2O_2 + Fe^{2+} \rightarrow Fe^{3+} + OH^- + {}^{\bullet}OH \qquad (1)$$

The oxidation of organics by $^{\bullet}OH$ generated from Fenton's reagent is relatively efficient, but this process suffers from several drawbacks that decrease the process efficiency; the most

important ones being: (i) the use of relatively high amounts of chemicals (reagent cost) [22], (ii) production of ferric hydroxide sludge [14] and (iii) involvement of wasting reactions between $^{\bullet}OH$ and Fenton's reagent due to the high concentrations of H_2O_2 and Fe^{2+} in the reaction medium [22]. More recently, a technology called electro-Fenton process [23-29] has been developed in order to overcome these drawbacks. Electro-Fenton process takes advantages of electrochemistry by generating H_2O_2 in situ from two-electron reduction of dissolved O_2 on a suitable cathode. To start the process, a catalytic amount of a ferrous iron salt is added to the solution as catalyst (Fe^{2+}) source [23] and then these ions are electrocatalytically regenerated from reduction of Fe^{3+} ions issued from Fenton's reaction (Eq. (1)). Thus, $^{\bullet}OH$ radicals produced through electrocatalytically generated Fenton's reagent (H_2O_2 + Fe^{2+}) in the bulk react quickly with organic pollutants that are hydroxylated and finally destroyed [24-27]. The efficiency of the electro-Fenton process depends on several operating parameters such as applied current, catalyst concentration, electrode material, solution pH, etc. [22, 24, 30-34]. Among these parameters, the role of the cathode material is crucial for the efficiency of electro-Fenton process since it determines the yield of H_2O_2 which in its turn influences the generation rate of $^{\bullet}OH$ according to the Eq. (1) [35-38]. The increase in concentration of H_2O_2 leads to the rise in $^{\bullet}OH$ generation rate according to the Fenton reaction (Eq. (1)) and finally the destruction of contaminants is enhanced. Therefore, this work aims at investigating and comparing the effectiveness of three cathode materials: stainless steel, carbon felt and carbon sponge with 5 different ppi in the electro-Fenton process always using platinum electrode as anode.

A systematic study of the effect of anode material on the electro-Fenton process has been already reported [39, 40]. The present study focuses on the effect of cathode material on the efficiency of electro-Fenton process. Therefore, the comparative efficiency of different cathode material commonly used, such as stainless steel, carbon felt and carbon sponge of

five different porosities (as a new cathode material), was performed based on the oxidative degradation and mineralization of a target pollutant: the sulfamethazine (SMT). SMT belongs to the group of sulfonamide pharmaceuticals widely used as antibacterial drugs and food additives in livestock production and is one of the most frequently used sulphonamides. As a consequence, it is widely present in natural water systems [40-42]. It has been observed that SMT represents toxic effects to daphnia magna [43], fertility effects in mice [44] and thyroid hormone homeostasis in rats [45]. We therefore selected this drug as a model pollutant to test the performance of different cathode material in terms of production of H_2O_2 generation ability, capacity of oxidation and mineralization as a function of applied current, the main parameter in electro-Fenton process.

2. Experimental Section

2.1 Chemicals

The model molecule SMT ($C_{12}H_{14}N_4O_2S$, 4-amino-*N*-(4,6-dimethylpyrimidin-2-yl) benzene-1-sulfonamide) was a sigma Aldrich product (≥ 99% purity) and used without further purification. Methanol and H_3PO_4 used in the preparation of HPLC eluents, and Na_2SO_4 (> 99% purity) employed as supporting electrolyte, were supplied by Sigma-Aldrich and Fluka. $FeSO_4{\cdot}7H_2O$ (99% purity) used as source of ferrous iron (catalyst), $TiCl_4$ (99.9%) and H_2SO_4 (98%) used to prepare the titanium reagent for H_2O_2 analysis were obtained from Acros. HPLC eluents and SMT working solutions were prepared with ultra-pure water obtained from a Millipore Milli-Q system with resistivity > 18 MΩ cm at room temperature. Potassium hydrogen phthalate (99.5%) used for total organic carbon analyzer (TOC) calibration was purchased from Shimadzu, France.

2.2. Electrolytic system

The experiments were carried out in a 250 mL electrolytic cell containing a platinum (Pt) anode and the given cathode, all of 6 cm × 3.5 cm geometric surface area. The Pt anode was purchased from PLATECXIS (France) whereas the cathodes were provided by different companies: carbon felt (MERSEN, France, density 0.08 g cm^{-3}, surface area (via nitrogen) 0.7 m^2/g); different pore size carbon sponges (reticulated vitreous carbon, ElectroCell Europe, Denmark, 0.050 g cm^{-3}, with 30, 45, 60, 80 and 100 ppi (pores per linear inch) that that correspond respectively to 17.1, 25.6, 34.2, 45.6 and 57.0 cm^2/cm^3), stainless steel (Goodfellow, France). The thickness of cathodes was: stainless steel: 2 mm, carbon felt: 5 mm, carbon sponge: 8 mm. Spacing of electrodes was 2.5 cm. SEM images and BET surfaces of these carbon electrodes as well as the characteristics provided by marketing companies can be found in the Supplementary Materials Section, SM-1 and SM-2.
A Hameg HM8040 triple power supply was used to monitor the electrochemical cell which is equipped with a magnetic stirrer to homogenize the solution.

First, the capacity of H_2O_2 production of each cathode relative to the oxygen reduction reaction was monitored and measured during the electrolysis of a 50 mM Na_2SO_4 aqueous solution adjusted at pH 3. Compressed air was continuously bubbled through the solution to provide the oxygen needed for H_2O_2 generation. The experimental trials were conducted at six different currents: 50, 100, 200, 300, 400 and 500 mA.

Similarly, the electrolysis of the SMT solutions was performed in a 250 mL electrochemical cell. Oxidation of target pollutant SMT was carried out at room temperature and at pH = 3, the optimal value for electro-Fenton process [24, 26, 46]. The pH was measured with a CyberScan pH 1500 pH-meter from Eutech Instruments. The experiments were performed under current-controlled electrolysis conditions, at various constant currents from 50 to 500 mA for electrooxidation and mineralization trials. Aqueous solutions containing 0.2 mM (28.8 mg L^{-1}) SMT and 50 mM Na_2SO_4 (supporting electrolyte) and 0.2 mM Fe^{2+} (catalyst) were

used for electrooxidation and mineralization experiments. Samples (20 µL for degradation kinetics and 3 mL for mineralization measurements) were withdrawn at pre-set time intervals in order to assess the concentration decay kinetics of SMT as well as the mineralization rate of treated solutions as a function current and electrolysis time.

The solution pH was monitored during the electrolysis; it never varied by more than 0.2 unit and no formation of sludge was observed. The stability of the cathodes was inspected visually and no change could be observed, it remained mechanically stable. In addition, the cathode was rinsed and immersed in a hydrochloric acid solution to remove any possible iron hydroxide precipitates. With this treatment the cathode could be reused for many experiments without any loss of performance.

2.3. Analytical procedures

The evolution of hydrogen peroxide during electrolysis was monitored by following the concentration of the complex formed between H_2O_2 and Ti^{4+}. The kinetics of H_2O_2 generation was established by withdrawing aliquots of 5 mL at given time scales that were introduced in a flask of 25 mL. In each aliquot 2 mL of $TiCl_4$ solution were added; they were prepared previously in 1 M H_2SO_4: 10 mL $TiCl_4$ in 1 L of 1 M H_2SO_4 + 2 mL of concentrated H_2SO_4 (18 M) and the final volume was completed to 25 mL with the pure water. Then the sample was measured at the maximum absorption wave length (423 nm) in a quartz vessel of 1 cm optical path. The absorption coefficient of the complex formed between H_2O_2 and Ti^{4+} was calculated from the slope of the calibration curve prepared with standard H_2O_2 solutions. Finally, the concentration of H_2O_2 was determined from the calibration curve according to the Beer-Lambert law using A Perkin-Elmer Lambda 10 UV/Vis spectrometer.

The time course decay of the SMT concentration during its electrooxidation was followed by a reversed phase HPLC using a Merck Lachrom chromatograph equipped with a quaternary pump L-7100, fitted with a Purospher RP 18, 5 µm, 25 cm x 4.6 mm (id) column at 40°C and

coupled with a L-7455 DAD detector selected at optimum wave length of 244 nm. The analysis of SMT decay was carried out isocratically with a mobile phase composed of methanol/phosphoric acid (1%) 90:10 (v/v) at a flow rate of 0.8 mL min^{-1}. Under these conditions, SMT showed a well-defined peak at retention time of 13.8 min. Samples of 20 µL were injected into the HPLC and measurements were controlled through EZ-Chrom Elite 3.1 software.

The extent of mineralization of electrolyzed solutions during the electro-Fenton treatment of SMT was assessed from the abatement of their TOC value, determined on a Shimadzu TOC-V_{CSH} analyzer according to the thermal catalytic oxidation principle. The carrying gas was oxygen with a flow rate of 150 mL min^{-1}. The temperature in the oven was 680 ^{o}C. Platinum was used as catalyst in order to carry out the combustion reaction at this temperature. Calibration of the TOC analyzer was done with potassium hydrogen phthalate standards.

3. Results and discussion

During the electro-Fenton process, the Fenton's reagent (which leads to the formation of the main oxidizing agent, $^{\bullet}OH$), is generated on the cathode surface; therefore its nature plays a crucial role for the effective destruction of organic pollutants. In the following parts, the experimental data obtained with different cathodes will be presented, namely: carbon sponge of five different porosities, carbon felt, and stainless steel. The production rate of H_2O_2 is a limiting parameter in electro-Fenton process. It strongly depends on the nature of cathode material but its optimum production conditions differ from those for the degradation of SMT. Therefore, in a first step, the ability of each cathode material to generate H_2O_2 was determined by analyzing the concentration of this species. The degradation kinetics and mineralization experiments were then performed using platinum as anode for all the cathodes studied.

3.1. Dosage of H_2O_2 in different electrolytic cells

Fig. 1 shows the evolution of the concentration of H_2O_2 with time for the carbon sponge cathodes of 45 and 80 ppi (pores per linear inch) porosities. The production of H_2O_2 starts when the current begins to flow through the cell due to the electrochemical reduction of dissolved oxygen, (Eq. (2)). It is high at the beginning of the electrolysis until it reaches a plateau and then remains almost constant. The plateau appears when the production rate of H_2O_2 (Eq. (2)) at cathode equals the rate of its destruction by thermal decomposition (Eq. (3)) and electrochemical oxidation (Eq. (4)) [24, 47].

$$O_2 + 2H^+ + 2e^- \rightarrow H_2O_2 \quad (2)$$

$$2H_2O_2 \rightarrow O_2 + 2H_2O \quad (3)$$

$$H_2O_2 \rightarrow HO_2^{\bullet} + H^+ + e^- \quad (4)$$

The evolution of H_2O_2 is very fast because it is mainly formed during the first 20 min and the plateau is reached within 1 h for lower (50, 100 and 200 mA) and within 40 min for higher (300-500 mA) current values. In general, the plateau of H_2O_2 concentration is reached earlier for carbon sponge of 45 ppi (Fig. 1a) than for 80 ppi porosity (Fig. 1b). More interestingly, carbon sponge of 45 ppi provides higher amounts of H_2O_2 than the 80 ppi porosity, owing to its more favorable macrostructure which provides better mass transport conditions. The maximal concentration of H_2O_2 production for both cathodes is reached at 100 mA whereas higher current values led to lower production due to the enhancement of the rate of side reactions (Eq. (5)) [24, 48] that compete with H_2O_2 generation (Eq. (2)), but also Eqs. (3) and (4) that consume H_2O_2. Therefore, the maximal H_2O_2 concentrations in the electrolytic cell were 3.5 mM (119 mg L^{-1}) and 2.4 mM (81.6 mg L^{-1}) for 45 and 80 ppi carbon sponge cathodes, respectively.

$$O_2 + 4H^+ + 4e^- \rightarrow 2H_2O \quad (5)$$

To compare with the generation H_2O_2 on carbon sponge, the same experiments were performed with two other cathodes: carbon felt and stainless steel; the results are depicted on the Fig. 2. As before, the amount of H_2O_2 produced was improved when the applied current increased from 50 to 100 mA and then slowed down for high currents. A very large amounts of H_2O_2 is produced at the early stage of electrolysis and, depending on the current applied, a plateau is attained from 20 min to 1 h. The capacity of the carbon felt cathode for H_2O_2 production was much lower than that of the carbon sponge, the maximal concentration accumulated for the optimal current of 100 mA being 1.2 mM (45.2 mg L^{-1}); 2.6 times lower than the 45 ppi carbon sponge. As for the stainless steel cathode, it provided very low H_2O_2 concentrations for currents of 50 and 100 mA and its concentration could not be quantified at higher currents due to the very small amounts generated and to the fast oxidation at the anode according to the Eq. (4).

3.2. The effect of current and cathode material on the degradation rate of SMT

To evaluate the effect of cathode material on the efficiency of the electro-Fenton process, the oxidative degradation of SMT was performed in an electrolytic cell of 250 mL at different current values. Samples were withdrawn at regular intervals and analyzed by HPLC. Fig. 3 shows the effect of the current on the kinetics of SMT oxidative degradation using carbon sponge cathodes of different porosity (30, 45, 60, 80 and 100 ppi). Clearly the rate of degradation of SMT increases with current as the result of higher $^{\bullet}OH$ production due to the enhanced rates of the electrochemical reactions for H_2O_2 and Fe^{2+} generation in cathode and chemically adsorbed $^{\bullet}OH$ radicals on the anode (Eq. (6)) including the regeneration of-Fe^{2+}.

Analysis of the curves of concentration decay indicates that the oxidative degradation of SMT is always governed by pseudo first order reaction kinetics. In fact, all the tested cathodes exhibit an excellent efficiency for degradation without any significant differences observed

between them. The degradation rate is the lowest with the 30 ppi cathode, it increases for 45 ppi close to 60 ppi and it decreases slightly for 80 and 100 ppi. An optimal current value is attained at 300-400 mA for the degradation efficiency of SMT while the maximum concentration of H_2O_2 is reached at 100 mA as discussed above (sub-section 3.1). These results can be explained by two facts: (i) H_2O_2 reacts with Fe^{2+} according to the Eq. (1) as it is formed; consequently it is not accumulated in the solution avoiding its thermal or electrochemical decomposition reactions, (ii) there is an additional contribution to the oxidation of SMT: heterogeneous $^{\bullet}OH$ radicals (formed by anodic oxidation of water according to the Eq. (6)), particularly at high current values. Although Pt($^{\bullet}OH$) [24] is chemically adsorbed on the anode surface, it can oxidize SMT molecules in its vicinity.

$$Pt + H_2O \rightarrow Pt(^{\bullet}OH) + H^+ + e^- \quad (6)$$

On the other hand, the degradation kinetics of SMT is progressively slowed down when increasing current value beyond 300-400 mA (the difference between 300 and 400 mA is very small). These values are gathered in Table 1.

This fact is generally observed in EAOPs and can be explained by the increase of wasting effect of parasitic reactions that commonly occur during the electrochemical advanced oxidation such as: (i) H_2 evolution at cathode which competes with 2-electron O_2 reduction to H_2O_2 (Eq. (2)), (ii) reduction of H_2O_2 at the cathode (Eq. (7)) [49], (iii) O_2 evolution at anode which compete with generation of Pt($^{\bullet}OH$) (Eq. (6)) and (iv) dimerization of $^{\bullet}OH$ (Eq. (8)) at high concentration [24].

$$H_2O_2 + 2\ H^+ + 2\ e^- \rightarrow 2\ H_2O \quad (7)$$

$$2\ ^{\bullet}OH \rightarrow H_2O_2 \quad (8)$$

For comparison, the effect of current on oxidation of SMT with carbon felt and stainless steel cathodes is presented in Fig. 4. The rate of SMT degradation increases with applied current from 50 to 200-300 mA where the limit of oxidation rate is attained. Then it decreases significantly from 300 to 500 mA (Fig. 4a). The degradation kinetics is significantly slower compared to Pt/carbon sponge cell that presents a higher production rate of H_2O_2. The experiments performed with a stainless steel cathode reveal a strongly different behavior (Fig. 4b) with a very slow SMT degradation kinetics. The concentration of SMT decays with time according to pseudo first order reaction kinetics but at the contrary to carbon sponge or carbon felt cathodes, all the curves present smaller slopes indicating a slow production of H_2O_2 in the solution. In this case, the degradation of SMT occurs mostly by anodic oxidation (through Pt($^{\bullet}$OH) produced at anode surface according to the equation (6)) and the limit of optimal current is attained at 300-400 mA. Also in all cases the complete oxidation of SMT requires significantly more time; it is still present in the solution after a 90 min electrolysis even at the most effective current values.

In order to summarize the performance of cathodes under examination, the values of apparent rate constants for the oxidative degradation of SMT obtained from semi-logarithmic plots ln (C_0/C) = f (t), assuming pseudo-first order reaction kinetics, are gathered in Table 1. The rate constants increase with the currents until an optimal value. The optimal current value for which the highest rate constant is observed depends to the cathode material. It is attained at 300 – 400 mA for carbon sponge of 30 – 60 ppi, 200 – 300 mA for carbon sponge of 80 – 100 ppi and carbon felt, and 300 mA for stainless steel cathodes.

Based on the obtained results, the best cathode for degradation of SMT was the carbon sponge of 45 ppi exhibiting excellent removal rates. If one excludes the inefficient SS, the lowest rate constants were obtained with 30 and 100 ppi carbon sponge. On the other side, all the carbon sponge cathodes performed better than carbon felt. The stainless steel cathode provides poor

capacity for the oxidation of SMT due to its very low production of hydroxyl radicals because of its very small specific surface area that contrasts with the carbon based cathodes with large surface area (owing to their 3D structure).

Moreover, the results showed a significant difference between carbon sponge and carbon felt. This difference can be explained by considering the hydrodynamic conditions in the bulk. Although the carbon felt is a very porous material with a large specific surface area than carbon sponge (as can be seen from BET surface analysis (SM-1 and Fig. SM-1) and SEM images(SM-2), its denser physical structure hampers the mass transfer to the depth of the cathode. In the same way one can explain the difference rate constants of degradation observed between carbon sponge cathodes of different porosity; degradation capacity increases from 30 ppi (structure close to carbon felt) to 45 ppi owing to the favorable mass transport conditions, then decreases slightly for 60 ppi and more strongly for 80 and 100 ppi porosities due to the decrease of specific surface area.

3.3. Efficiency of different cathodes for mineralization of SMT solution

Mineralization experiments were performed to estimate the oxidizing power of the electro-Fenton process with different cathodes. Experiments were conducted under the same conditions as the degradation experiments by applying currents of 50, 100, 300 and 500 mA. The results obtained in terms of TOC removal efficiency for five carbon sponge cathodes are given in the Fig. 5. The efficiency of TOC abatement follows a similar trend as for oxidation experiments. The degree of TOC removal was the lowest for 30 ppi carbon sponge cathode; it increased for 45 ppi being almost same for 60 ppi and then decreased for 80 and 100 ppi porosities. The maximum TOC removal of 91.1% was achieved with the 45 ppi cathode at the optimal current value of 300 mA. The TOC removal curves obtained at 500 mA are almost identical to those obtained at 300 mA, highlighting the fact that no enhancement in mineralization efficiency obtained for currents above 300 mA.

Conversely, lower mineralization efficiencies of SMT solution (in terms of TOC removal percentage) were obtained with carbon felt and stainless steel cathodes (Fig. 6). The maximum TOC abatement value was 55.7% (Fig. 6a) and 37.1 % (Fig. 6b) for carbon felt and stainless steel cathodes, respectively, at 300 mA. It can be noticed that the curves of mineralization kinetics are closer each to others inversely to carbon sponge cathodes. This behavior can be explained by a high amount of H_2O_2 production even at lower currents. At currents over 300 mA, the increase in H_2O_2 production is hampered by intensification of wasting reactions (5) – (8) discussed above. The extent of mineralization attained with stainless steel cathode was significantly lower compared to carbonaceous cathodes due to its poorer ability to produce H_2O_2.

The results depicted on the Table 2 show that the most effective cathode both for SMT oxidation and mineralization is the 45 ppi carbon sponge. However, carbon sponge of 60 ppi provided results close to that of the 45 ppi carbon sponge cathode. The 80 and 100 ppi carbon sponges showed lesser performance compared to the 45 ppi cathode. It is worth noticing that all carbon sponge cathodes provided remarkably better efficiency in electro-Fenton process than carbon felt and stainless steel cathodes. TOC abatement with stainless steel was the lowest whereas carbon felt exhibited mediate TOC removal extent. High surface area and rigid and porous structure of carbon sponge provide very good mass transport conditions leading to higher amounts of H_2O_2 production and faster Fe^{2+} (catalyst) electro-regeneration, resulting in high mineralization efficiencies. Stainless steel does not provide interesting mineralization degrees because of its small surface area and poor H_2O_2 production ability.

The mineralization current efficiency (MCE%) is an important parameter of electrochemical processes. In order to compare the current efficiency of different cathode material, this parameter was determined for each cathode according to the Eq. (9) [50],

$$\text{MCE}\ (\%) = \frac{n\,F\,V_s\,\Delta(\text{TOC})_{exp}}{4.32\times10^{7}\,m\,I\,t} \times 100 \qquad (9)$$

where I is the current (in A), F is the Faraday constant (96,487 C mol^{-1}), V_s is the solution volume (in L), $\Delta(TOC)_{exp}$ is the experimental TOC decay (in mg L^{-1}), 4.32×10^7 is a conversion factor to homogenize units (=3600 s h^{-1} × 12 000 mg of C mol^{-1}), m is the number of carbon atoms of SMT (= 12) and t is the electrolysis time (h). The number of electrons n consumed per SMT molecule during the mineralization process was taken as 84, according to Eq. (10).

$$C_{12}H_{14}N_4O_2S + 38\ H_2O \rightarrow 12CO_2 + 4NO_3^- + SO_4^{2-} + 90\ H^+ + 84\ e^- \qquad (10)$$

This reaction was written according to the results obtained by Sopaj et al. [40] in a previous report noting the predominant formation of ammonium compared to ammonia.

The results depicted in Figs. (7) and (8) are obtained from corresponding mineralization data of the Figs. (5) and (6) respectively. As can be seen from Figs. (7) and (8), the initial MCE% values are relatively high for all cathodes at low currents and decrease at high currents and with time. As the electrolysis proceeds, there is less organic matter in the solution leading a decrease of the reaction rate with •OH and consequently of TOC removal rate. On the other hand, the low MCE% values for high currents can be related to the loss of electrical energy through side reactions such as hydrogen evolution reaction at the cathode and oxygen evolution reaction at the anode in addition of H_2O_2 decomposition on electrodes (Eqs. (4) and (8).

These results clearly show the superiority of the carbon sponge over carbon felt. The stainless steel appears as the less effective cathode material with a very low MCE% values at all currents as a consequence of its poor H_2O_2 generation ability and therefore its low •OH production. In this case, the mineralization occurs mainly at the surface of Pt anode which has

a low oxidation power. Obviously the most powerful cathode for mineralization (in term of TOC removal) of SMT solution is the 45 ppi carbon sponge leading the highest MCE% value at short electrolysis times; MCE% decreases at longer electrolysis times but remains always higher than the other cathodes materials under study.

4. Conclusions

The performance of different cathodes was compared during the oxidative degradation and mineralization of the aqueous solution of the SMT drug by electro-Fenton process. The ability of carbon sponges with different porosities, carbon felt and stainless steel cathodes to produce H_2O_2 was tested in an electrochemical cell with a Pt anode. Carbon sponge cathodes exhibited remarkably better results than carbon felt, the classical cathode for electro-Fenton process, which, in turn, provided significantly better results than the stainless steel cathode. Among the carbon sponge cathodes, the best results were achieved with the 45 ppi cathode. Among the carbon sponge cathode, the best results were achieved with the 45 ppi carbon sponge cathode. The better performance of carbon sponges and in particular that of the 45 ppi carbon sponge can be attributed to its favorable mass transport conditions. Its high specific surface area and high porosity allow very good circulation of the solution through this 3D cathode. Therefore molecular oxygen can easily reach its surface, promoting the generation of H_2O_2 which, in turn, can move freely towards the bulk of the solution where it reacts with Fe^{2+} to produce hydroxyl radicals. In contrast, the transport of O_2 and H_2O_2 in the mass of cathode is hampered in the case of carbon felt due to its more dense structure leading to lower H_2O_2 generation. At the contrary, of the above carbonaceous cathodes, stainless steel is a 2D material with a relatively small surface and low production of H_2O_2 leading very low $^{\bullet}OH$ concentration in the bulk solution and consequently poor oxidation/mineralization results for removal of SMT.

Acknowledgment

We are grateful to Dr. S. Gam Derouich and to Pr. J.-Y. Piquemal for the SEM images and the BET analysis, respectively.

Flamur Sopaj acknowledges the embassy of France in Kosovo for the PhD scholarship granted by the French government, which enabled the realization of this work.

References

[1] S.A. Snyder, P. Westerhoff, Y. Yoon, D.L. Sedlak, Pharmaceuticals, personal care products and endocrine disruptors in water: implication for water treatment, Environ. Eng. Sci. 20 (2003) 449-469.

[2] Directive 2008/32/EC of the European parliament and of the Council of 11 March 2008 amending Directive 2000/32/EC.

[3] S.K. Khetan, T.J. Collins, Human pharmaceuticals in the aquatic environment: a challenge to green chemistry, Chem. Rev. 107 (2007) 2319–2364.

[4] L. Feng, E.D. van Hullebusch, M.A. Rodrigo, G. Esposito, M.A. Oturan, Removal of residual anti-inflammatory and analgesic pharmaceuticals from aqueous systems by advanced oxidation processes. A review, Chem. Eng. J. 228 (2013) 944–964.

[5] S. Chiron, L. Comoretto, E. Rinaldi, V. Maurino, D. Vione, Pesticide by-products in the Rhone delta (Southern France). The case of 4-chloro-2-methylphenol and of its nitro derivative, Chemosphere 74 (2009) 599–604.

[6] L.R. Zimmerman, E.M. Thurman, K.C. Bastian, Detection of persistent organic pollutants in the Mississippi Delta using semipermeable membrane devices, Sci. Total Environ. 248 (2000) 169–179.

[7] S. Vasudevan, M.A. Oturan, Electrochemistry as cause and cure in water pollution. An overview, Environ. Chem. Lett. 12 (2014) 97–108.

[8] K. Kümmerer, Antibiotics in the environment – A review – Part I, Chemosphere 75 (2009) 417-434.

[9] M.M. Mortland, S. Shaobai, S.A. Boyd, Clay-organic complexes as adsorbents for phenol and chlorophenlos, Clays Clay Miner. 34 (1986) 581-585.

[10] J.L. Acero, F.J. Benitez, A.I. Leal, F.J. Real, F. Teva, Membrane filtration technologies applied to municipal secondary effluents for potential reuse, J. Hazard. Mater. 177 (2010) 390-398.

[11] M. Henze, M.C.M. van Loosdrecht, C.A. Ekama, D. Brdjanovic (Eds), Biological Wastewater Treatment: Principles, Modeling and Design, IWA Publishing, London 2008, ISBN: 1843391880.

[12] D. Fatta-Kassinos, D.D. Dionysiou, K. Kümmerer (Eds.), Advanced Treatment Technologies for Urban Wastewater Reuse, The Handbook of Environmental Chemistry, Vol. 45, Springer, 2016, doi: 10.1007/698_2015_449.

[13] V.J.P. Vilar, C.C. Amorim, E. Brillas, G.L. Puma, S. Malato, D.D. Dionysiou, AOPs: recent advances to overcome barriers in the treatment of water, wastewater and air, Environ. Sci. Pollut. Res. 7 (2017) 5987-5990.

[14] S. Esplugas, J. Gimenez, S. Contreras, E. Pascual, M. Rodriguez, Comparison of different advanced oxidation processes for phenol degradation, Water Res. 36 (2002) 1034-1042.

[15] E. Brillas, C.A. Martinez-Huitle, Decontamination of wastewater containing synthetic organic dyes by electrochemical methods. An updated review, Appl. Catal. B: Environ. 166-167 (2015), pp. 603-643.

[16] Taner Yonar, Kadir Kestioglu, Nuri Azbar, Treatability studies on domestic wastewater using UV/H_2O_2 process, Appl. Catal. B: Environ. 67 (2006) 223-228.

[17] María A. Fontecha-Cámara, Carlos Moreno-Castilla, María Victoria López-Ramón, Miguel A. Álvarez, Mixed iron oxides as Fenton catalysts for gallic acid removal from aqueous solutions, Appl. Catal. B: Environ.196 (2016) 207-215.

[18] Gamal M. S. ElShafei, A. M. Al-Sabagh, F. Z. Yehia, C. A. Philip, N.A. Moussa, Gh. Eshaq, A. E. ElMetwally, Metal oxychlorides as robust heterogeneous Fenton catalysts for the sonophotocatalytic degradation of 2-nitrophenol, Appl. Catal. B: Environ. 224 (2018) 681-691.

[19] J.J. Pignatello, E. Oliveros, A. MacKay, Advanced oxidation processes for organic contaminant destruction based on the Fenton reaction and related chemistry, Crit. Rev. Environ. Sci. Technol. 36 (2006) 1–84.

[20] M.A. Rodrigo, N. Oturan, M.A., Electrochemically assisted remediation of pesticides in soils and water: A review, Chem. Rev. 114 (2014) 8720-8745.

[21] E. Mousset, N. Oturan, M.A. Oturan, An unprecedented route of •OH radical reactivity: ipso-substitution with perhalogenocarbon compounds, Appl. Catal. B: Environ. 226 (2018) 135-156.

[22] M.A. Oturan, J.J. Aaron, Advanced oxidation processes in water/wastewater treatment: Principles and applications. A review, Crit. Rev. Environ. Sci. Technol. 44 (2014) 2577-2641.

[23] M.A. Oturan, An ecologically effective water treatment technique using electrochemically generated hydroxyl radicals for in situ destruction of organic pollutants: Application to herbicide 2.4-D, J. Appl. Electrochem. 30 (2000) 475-482.

[24] E. Brillas, I. Sirés, M.A. Oturan, Electro-Fenton process and related electrochemical technologies based on Fenton's reaction chemistry, Chem. Rev. 109 (2009) 6570-6631.

[25] I. Sirés, E. Brillas, M.A. Oturan, M.A. Rodrigo, M. Panizza, Electrochemical advanced oxidation processes: today and tomorrow. A review, Environ. Sci. Pollut. Res. 21 (2014) 8336-8367.

[26] Oturan N., Oturan M.A. Electro-Fenton Process: Background, New Developments and Applications. In: C.A. Martinez-Huitle, M.A. Rodrigo, O. Scialdone (Eds.), Electrochemical Water and Wastewater Treatment, Elsevier, Oxford (UK) and Cambridge (MA-USA), 2018, pp. 193-221, ISBN: 978-0-12-813160-2

[27] M. Zhou, M.A. Oturan, I. Sirés (Eds.), Electro-Fenton Process: New Trends and Scale-Up (ISBN: 978-981-10-6405-0), in: The Handbook of Environmental Chemistry, volume 61, 2017, Springer, ISSN: 1867-979X.

[28] S. Ben Hammouda, F. Fourcade, A. Assadi, I. Soutrel, N. Adhoum, A Amrane, L Monser, Effective heterogeneous electro-Fenton process for the degradation of a malodorous compound, indole, using iron loaded alginate beads as a reusable catalyst, Appl. Catal. B: Environ. 182 (2016) 47-58.

[29] A. Kesraoui-Abdessalem, N. Oturan, N. Bellakhal, M. Dachraoui, M. A. Oturan, Experimental design methodology applied to electro-Fenton treatment for degradation of herbicide chlortoluron, Appl. Catal. B: Environ. 78 (2008) 334-341.

[30] E. Guinea, J.A. Garrido, R.M. Rodriguez, P-L. Cabot, C. Arias, F. Centellas, E. Brillas, Degradation of the fluoroquinolone enrofloxacin by electrochemical advanced oxidation processes based on hydrogen peroxide electrogeneration, Electrochim. Acta 55 (2010) 2101-2115.

[31] M. Murati, N. Oturan, J-J. Aron, A. Dirany, B. Tussin, Z. Zdravkovski, M. Oturan, Degradation and mineralization of sulcotrione and mesotrione in aqueous medium by the electro-Fenton process: a kinetic study, Environ. Sci. Pollut. Res. 19 (2012) 1563-1573.

[32] P.V. Nidheesh, R. Gandhimathi, Trends in electro-Fenton process for water and wastewater treatment: An overview, Desalination 299 (2012) 1-15.

[33] M.A. Oturan, M.C. Edelahi, N. Oturan, K. El Kacemi, J-J. Aaron, Kinetics of oxidative degradation/mineralization pathways of the phenylurea herbicides diurion, monuron and fenuron in water during application of the electro-Fenton process, Appl. Catal. B: Environ. 97 (2010) 82-89.

[34] A. Lahkimi, M. Chaouch, N. Oturan, M.A. Oturan, Removal of textile dyes from water by electro-Fenton process, Environ. Chem. Lett. 5 (2007) 35-39.

[35] C-T. Wang, J-L. Hu, W-L. Chou, Y-M. Kuo, Removal of color from real dyeing wastewater by electro-Fenton technology using a three-dimensional graphite cathode, J. Hazard. Mater. 152 (2008) 601-606.

[36] M. Panizza, M.A. Oturan, Degradation of alizarine red by electro-Fenton process using a graphite-felt cathode, Electrochim. Acta 56 (2011) 7084-7087.

[37] M. Pimentel, N. Oturan, M. Dezotti, M.A. Oturan, Phenol degradation by advanced electrochemical oxidation process electro-Fenton using a carbon felt cathode, Appl. Catal. B: Environ. 83 (2008) 140-149.

[38] A. Özcan, Y. Sahin, A.S. Koparal, M.A. Oturan, Carbon sponge as a new cathode material for electro-Fenton process: Comparison with carbon felt cathode and application to degradation of synthetic dye basic blue 3 in aqueous medium, J. Electroanal. Chem. 616 (2008) 71-78.

[39] N. Borras, C. Arias, R. Oliver, E. Brillas, Mineralization of desmetryne by electrochemical advanced oxidation processes using a boron-doped diamond anode and an oxygen-diffusion cathode, Chemosphere 85 (2011) 1167-1175.

[40] F. Sopaj, N. Oturan, J. Pinson, F. Podvorica, M.A. Oturan, Effect of the anode materials on the efficiency of the electro-Fenton process for the mineralization of the antibiotic sulfamethazine, Appl. Catal. B: Environ. 199 (2016) 331-341.

[41] M-O. Aust, F. Godlinski, G.R. Travis, X. Hao, T.A. McAllister, P. Leinweber, S. Thiele-Bruhn, Distribution of sulfamethazine, chlorotetracycline and tylosin in manure and soil of

Canadian feedlots after subtherapeutic use in cattle, Environ. Pollut. 156 (2008) 1243-1251.

[42] Barhoumi N., Oturan N., Olvera-Vargas H., Brillas E., Gadri A., Ammar S., Oturan M.A. Pyrite as a sustainable catalyst in electro-Fenton process for improving oxidation of sulfamethazine. Kinetics, mechanism and toxicity assessment, Water Res. 94 (2016) 52-61.

[43] L.H.M.I.M. Santos, A.N. Araujo, A.F.A. Pena, C. Delure-Matos, M.C.B.S.M. Montenegro, Ecotoxicological aspects related to the presence of pharmaceuticals in the aquatic environment, J. Hazard. Mater. 175 (2010) 45-95.

[44] J.R. Reel, R.W. Tyl, A. Davis-Lawton, J.C. Lamb, Reproductive toxicity of sulfamethazine in Swiss CD-I mice during continuous breeding, Fundam. Appl. Toxicol. 18 (1992) 609-615.

[45] L.A. Poirier, D.R. Doerge, D.W. Gaylor, M.A. Miller, R.J Lorentzen, D.A. Casciano, F.F. Kadlubar, B.A. Schwetz, An FDA review of sulfamethazine toxicity, Regul. Toxicol. Pharma. 30 (1999) 217-222.

[46] M. Pimentel, N. Oturan, M. Dezotti, M.A. Oturan, Phenol degradation by advanced electrochemical oxidation process electro-Fenton using a carbon felt cathode, Appl. Catal. B: Environ. 83 (2008) 140-149.

[47] E. Brillas, R. M. Bastida, E. Llosa, and J. Casado, Electrochemical destruction of aniline and 4-chloroaniline for wastewater treatment using carbon-PTFE O2-fed cathode, J. Electrochem. Soc. 142 (1995) 1733-1741.

[48] P. C. Foller, R. T. Bombard, Processes for the production of mixtures of caustic soda and hydrogen peroxide via the reduction of oxygen, J. Appl. Electrochem. 25 (1995) 613-627.

[49] Z. Qiang, J-H. Chang, C-P Huang, Electrochemical generation of hydrogen peroxide from dissolved oxygen in acidic solutions, Water Research. 36 (2002) 85-94.

[50] M. Panizza, M. A. Oturan, Degradation of Alizarin Red by electro-Fenton process using a graphite-felt cathode, Electrochimica Acta 56 (2011) 7084-7087.

Table Captions

Table 1. Values of apparent rate constants (k_{app}) observed during degradation of SMT by electro-Fenton process as a function of the cathode material and applied current.

I (mA)	k_{app} (min^{-1})						
	CS[1]30 ppi	CS45 ppi	CS60 ppi	CS80 ppi	CS100 ppi	CF[2]	SS[3]
50	0.11	0.19	0.19	0.19	0.19	0.06	0.03
100	0.22	0.34	0.28	0.28	0.29	0.07	0.04
200	0.36	0.49	0.43	0.42	0.38	0.14	0.06
300	0.41	0.60	0.50	0.43	0.39	0.16	0.07
400	0.43	0.61	0.48	0.41	0.37	0.11	0.07
500	0.37	0.57	0.38	0.33	0.31	0.09	0.06

[1] carbon sponge, [2] carbon felt, [3] stainless steel

Table 2. TOC removal degrees obtained with different cathodes during electro-Fenton treatment of 0.1 mM SMT aqueous solution as a function of applied current.

I (mA)	% TOC removal 8h						
	CS[1]30 ppi	CS45 ppi	CS60 ppi	CS80 ppi	CS100 ppi	CF[2]	SS[3]
50	46.5	63.4	62.1	54.8	54.1	43.4	20.9
100	67.7	76.6	74.3	69.7	69.7	49.7	29.9
300	80.2	91.1	91.2	83.9	82.6	55.6	37.2
500	79.5	90.1	83.6	83.3	80.7	56.6	41.2

[1] carbon sponge, [2] carbon felt [3] stainless steel

Figure captions

Figure 1. Evolution of H_2O_2 concentration during electrolysis of O_2 in the cells equipped with Pt anode and carbon sponge cathodes of (a) 45 ppi and (b) 80 ppi porosities under continuous air bubbling conditions. V_s = 250 mL, [Na_2SO_4] = 50 mM, pH = 3.

Figure 2. Evolution of H_2O_2 concentration in the cells with carbon felt (a) and stainless steel (b) cathodes, under continuous air bubbling conditions. Anode: Pt, V_s = 250 mL, [Na_2SO_4] = 50 mM, pH = 3.

Figure 3. Effect of current on the degradation rate of SMT during electro-Fenton oxidation using Pt anode/carbon sponge (CS) cathode of different porosities: (a) Pt/CS-30 ppi, b) Pt/CS-45 ppi, c) Pt/CS-60 ppi, d) Pt/CS-80 ppi and e) Pt/CS-100 ppi. V_s = 250 mL, [SMT] = 0.2 mM, [Fe^{2+}] = 0.2 mM, [Na_2SO_4] = 50 mM, pH = 3.

Figure 4. Effect of current on the degradation kinetic of SMT in the (a) Pt /carbon felt cell and (b) Pt/stainless steel cell. V_s = 250 mL, [SMT] = 0.2 mM, [Fe^{2+}] = 0.2 mM, [Na_2SO_4] = 50 mM, pH = 3.

Figure 5. Effect of current on the mineralization of SMT in the Pt/Carbon sponge cell with different carbon sponge porosities: a) 30 ppi, b) 45 ppi, c) 60 ppi, d) 80 ppi, e) 100 ppi. V_s = 250 mL, [SMT] = 0.2 mM, [Fe^{2+}] = 0.2 mM, [Na_2SO_4] = 50 mM, pH = 3.

Figure 6. Effect of current on the mineralization of 0.2 mM SMT solutions in the a) Pt/Carbon felt cell, b) Pt/Stainless steel cell. V_s = 250 mL, [Fe^{2+}] = 0.2 mM, [Na_2SO_4] = 50 mM, pH = 3.

Figure 7. MCE% initial values and evolution with electrolysis time of carbon sponge cathodes of different porosities: (a) 30 ppi, (b) 45 ppi, (c) 60 ppi, (d) 80 ppi, (e) 100 ppi. V_s = 250 mL, [SMT] = 0.2 mM, [Fe^{2+}] = 0.2 mM, [Na_2SO_4] = 50 mM, pH = 3.

Figure 8. MCE% initial values and evolution with electrolysis time during mineralization of 0.2 mM SMT solutions in: Pt/Stainless (a) and Pt/Carbon felt (b) cells. V_s = 250 mL, [Fe^{2+}] = 0.2 mM, [Na_2SO_4] = 50 mM, pH = 3.

.

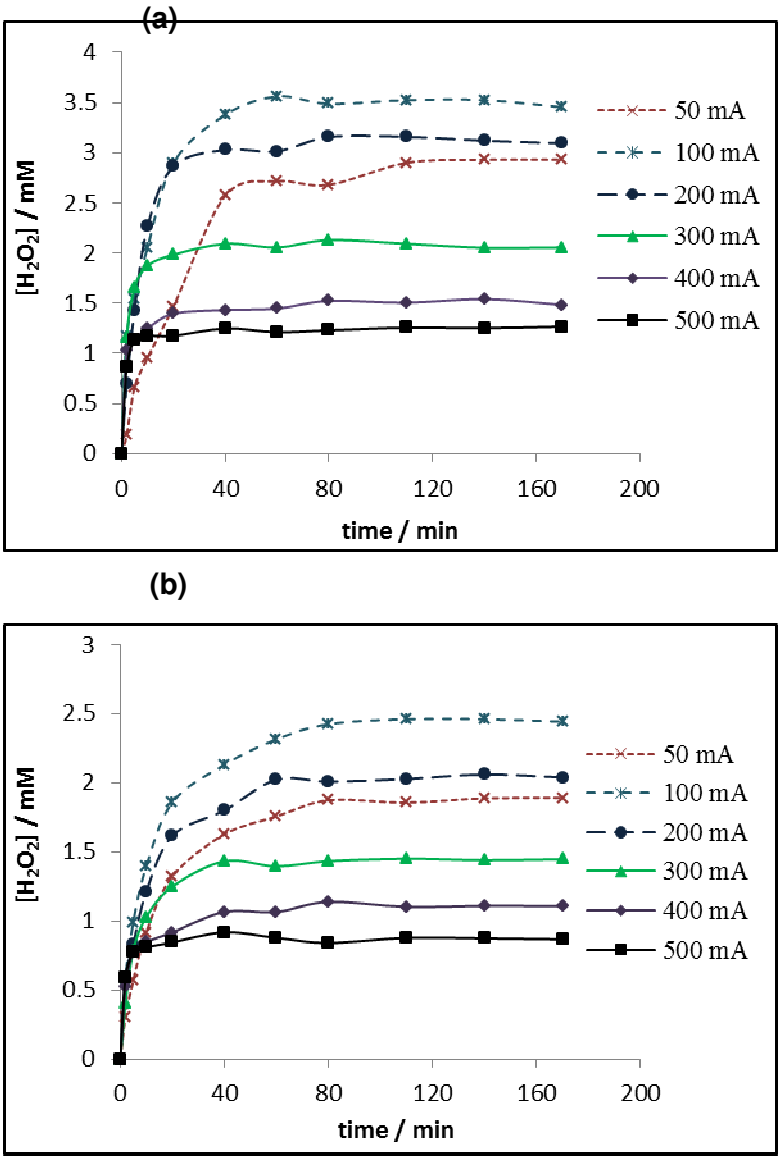
(a)
[H2O2] / mM
time / min
50 mA
100 mA
200 mA
300 mA
400 mA
500 mA
(b)
[H2O2] / mM
time / min
50 mA
100 mA
200 mA
300 mA
400 mA
500 mA

Figure 1

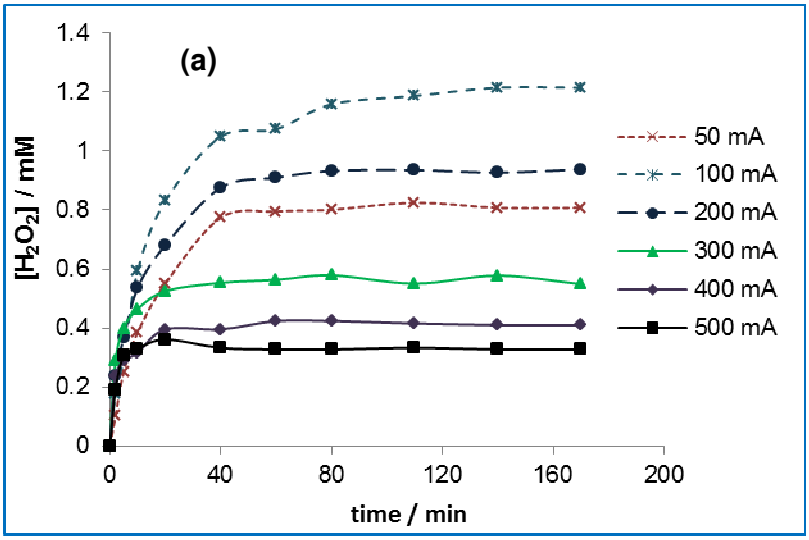
(a)
1.4
1.2
1
0.8
0.6
0.4
0.2
0
[H2O2] / mM
0
40
80
120
160
200
time / min
50 mA
100 mA
200 mA
300 mA
400 mA
500 mA

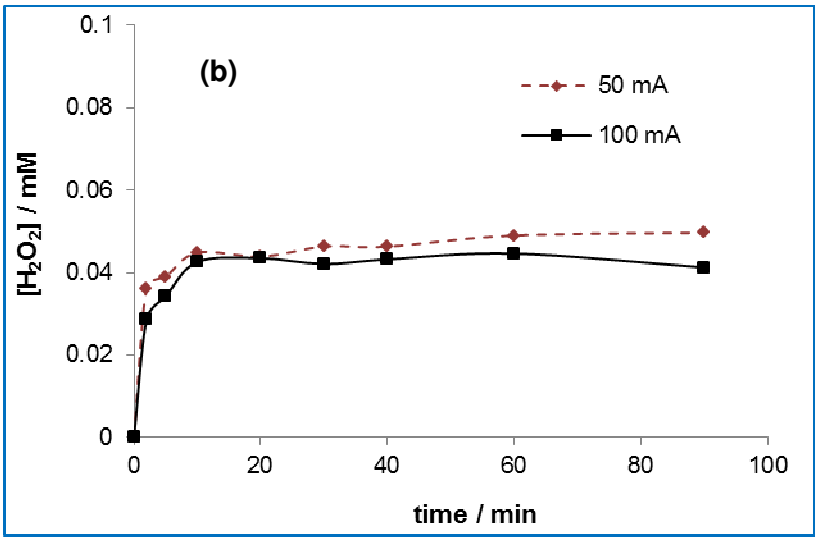
(b)
0.1
0.08
0.06
0.04
0.02
0
[H2O2] / mM
0
20
40
60
80
100
time / min
50 mA
100 mA

Figure 2

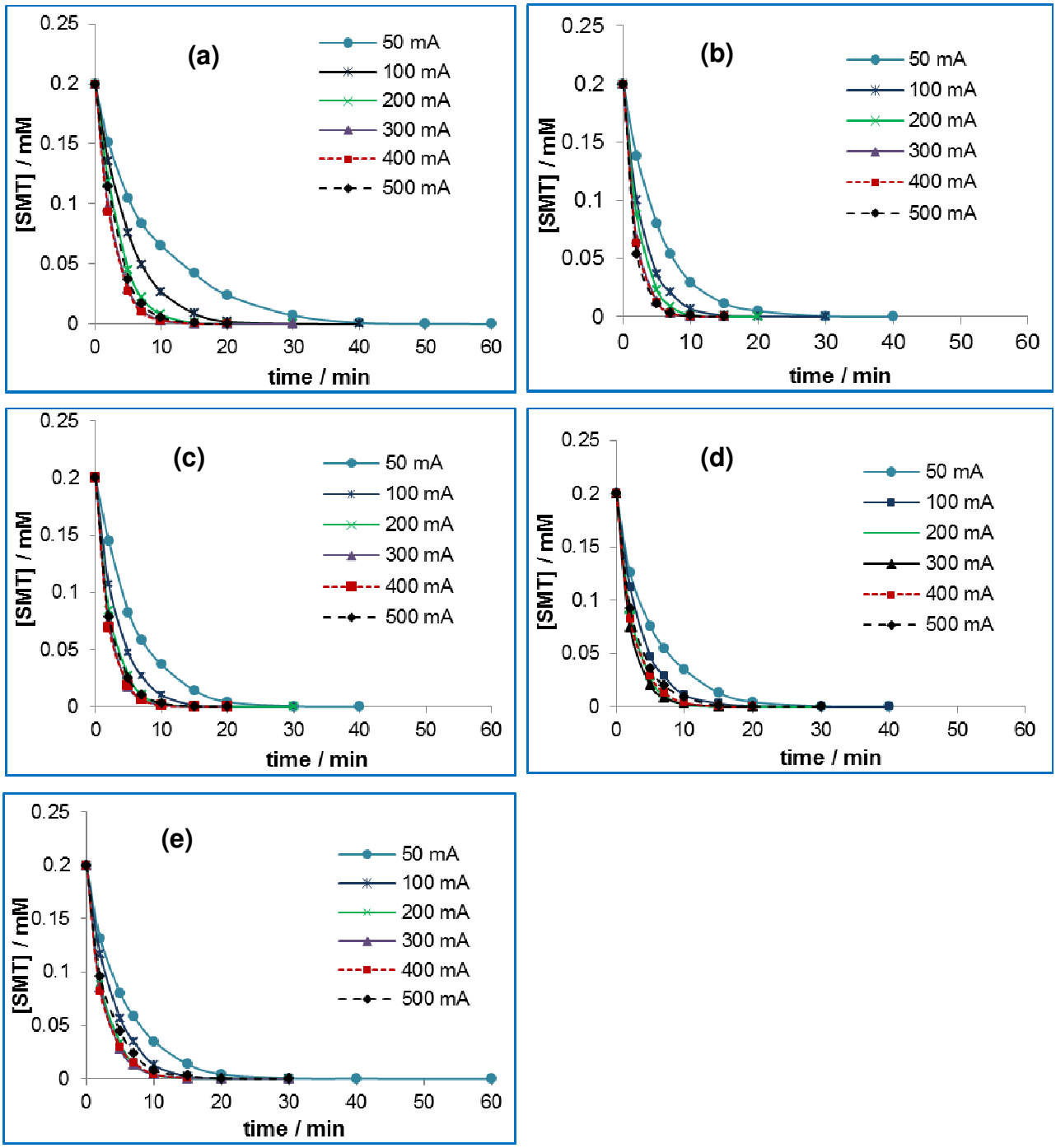
(a)
(b)
(c)
(d)
(e)
[SMT] / mM
time / min
50 mA
100 mA
200 mA
300 mA
400 mA
500 mA
0.25
0.2
0.15
0.1
0.05
0
0
10
20
30
40
50
60

Figure 3

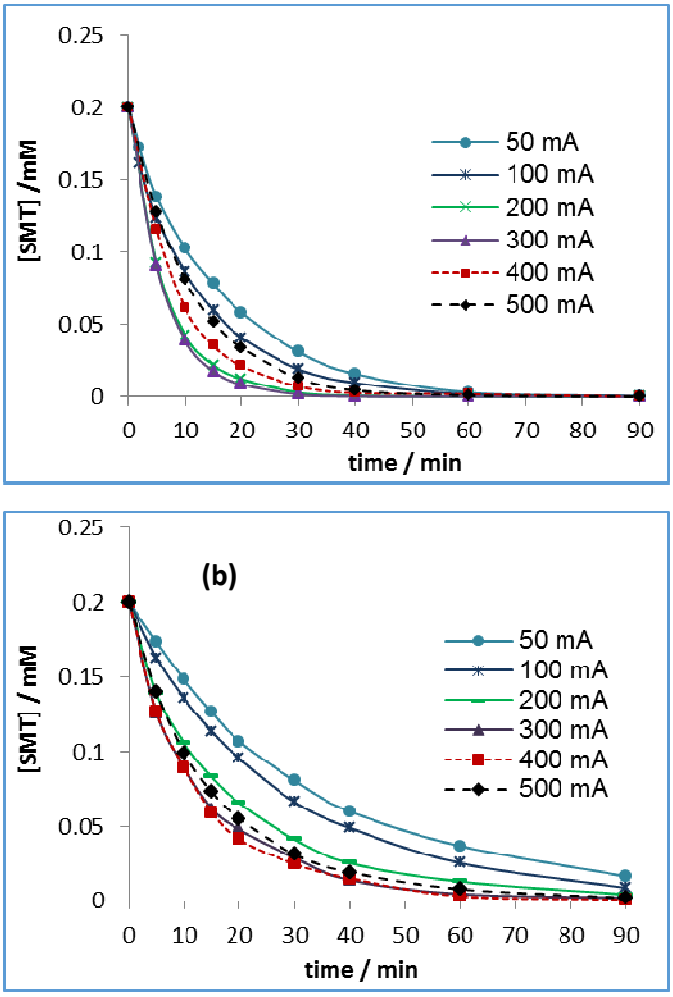
0.25
0.2
0.15
0.1
0.05
0
[SMT] /mM
0 10 20 30 40 50 60 70 80 90
time / min
50 mA
100 mA
200 mA
300 mA
400 mA
500 mA
(b)
0.25
0.2
0.15
0.1
0.05
0
[SMT] / mM
0 10 20 30 40 50 60 70 80 90
time / min
50 mA
100 mA
200 mA
300 mA
400 mA
500 mA

Figure 4

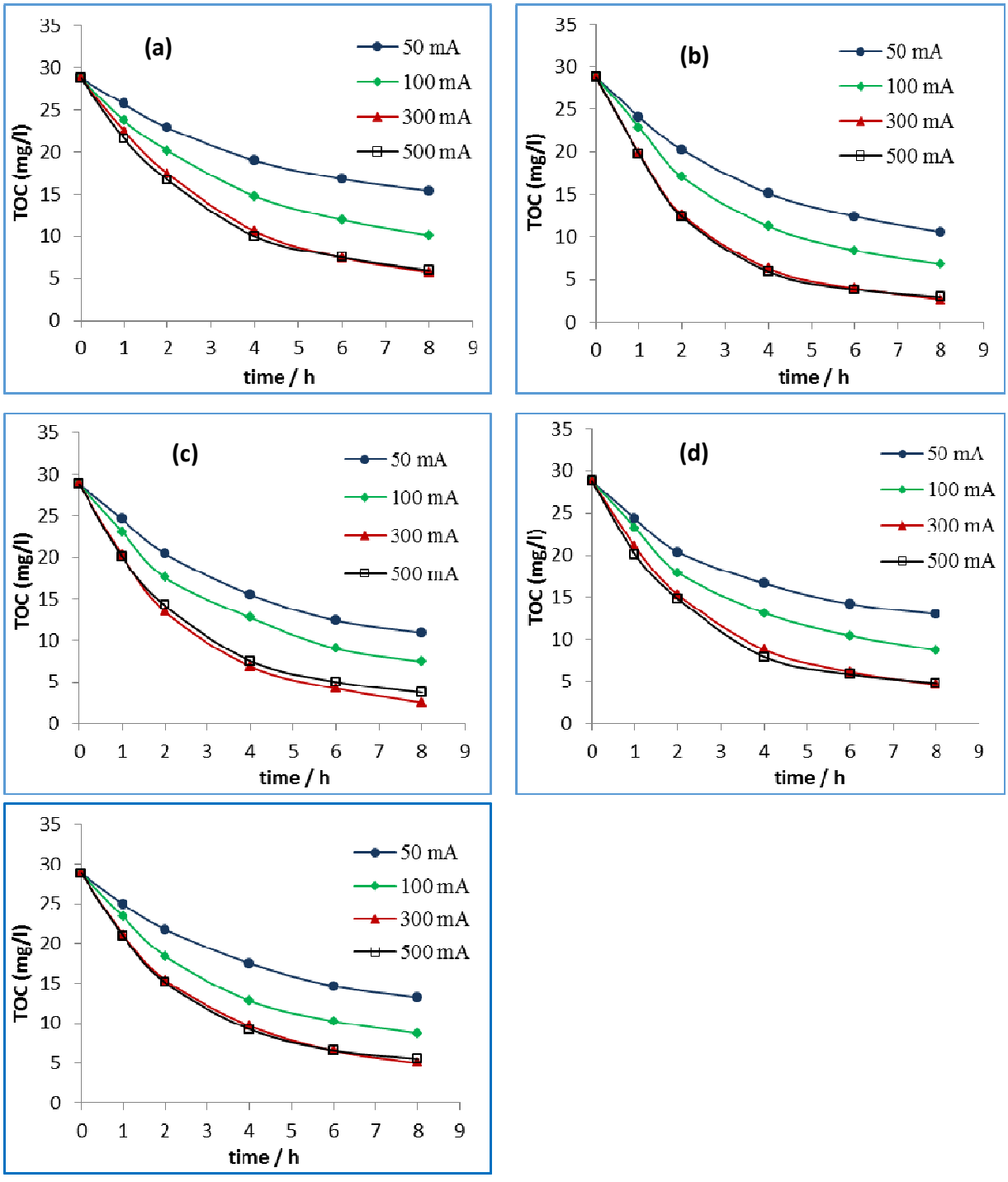

Figure 5

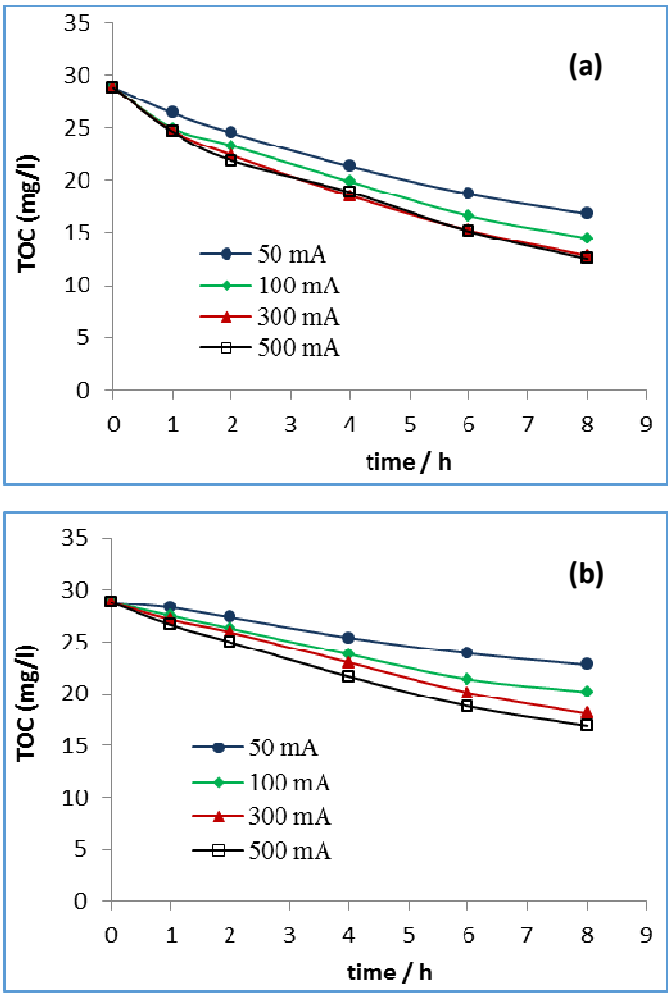
(a)
TOC (mg/l)
time / h
50 mA
100 mA
300 mA
500 mA
(b)
TOC (mg/l)
time / h
50 mA
100 mA
300 mA
500 mA

Figure 6

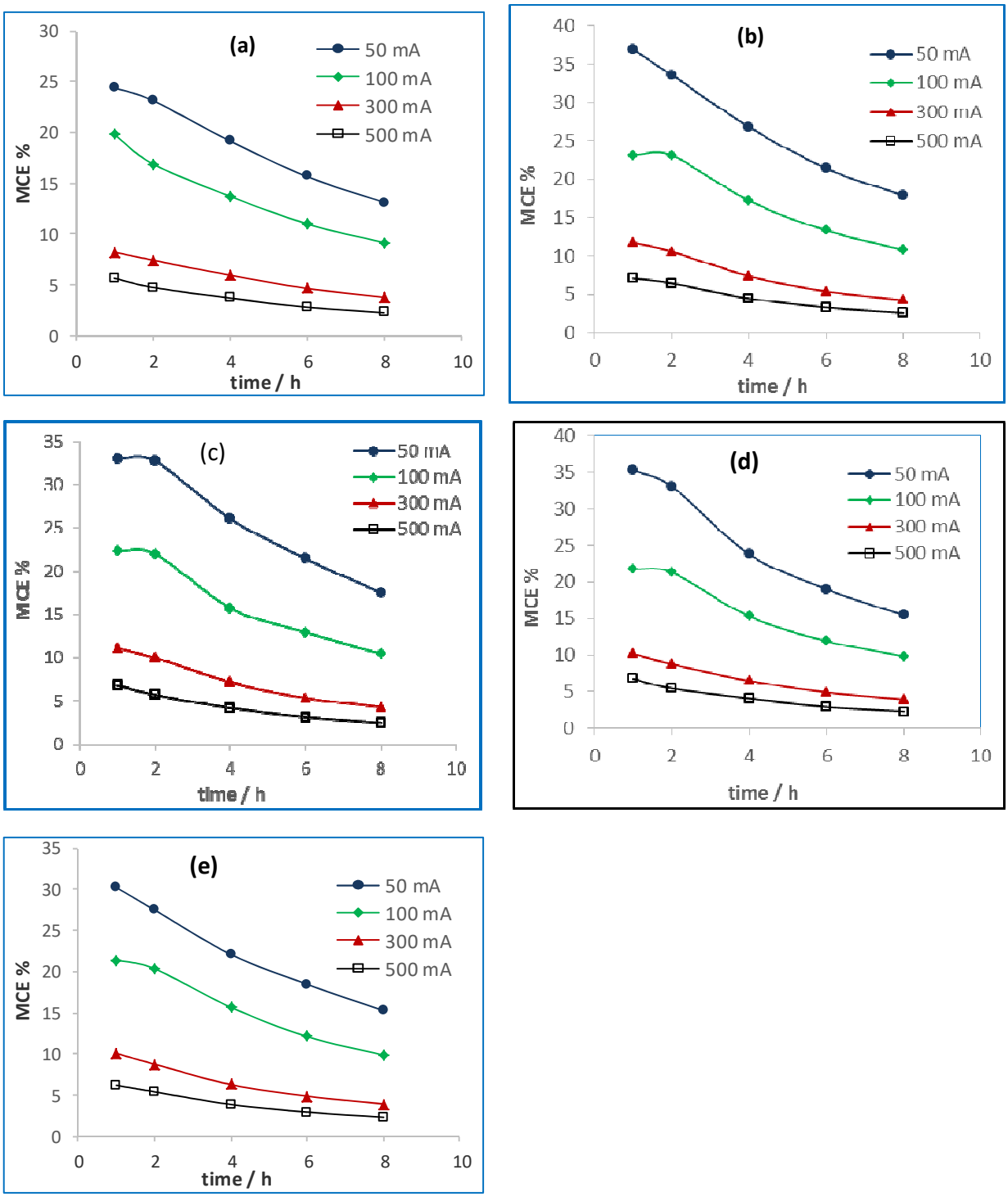
(a)
50 mA
100 mA
300 mA
500 mA
MCE %
time / h
(b)
50 mA
100 mA
300 mA
500 mA
MCE %
time / h
(c)
50 mA
100 mA
300 mA
500 mA
MCE %
time / h
(d)
50 mA
100 mA
300 mA
500 mA
MCE %
time / h
(e)
50 mA
100 mA
300 mA
500 mA
MCE %
time / h

Figure 7

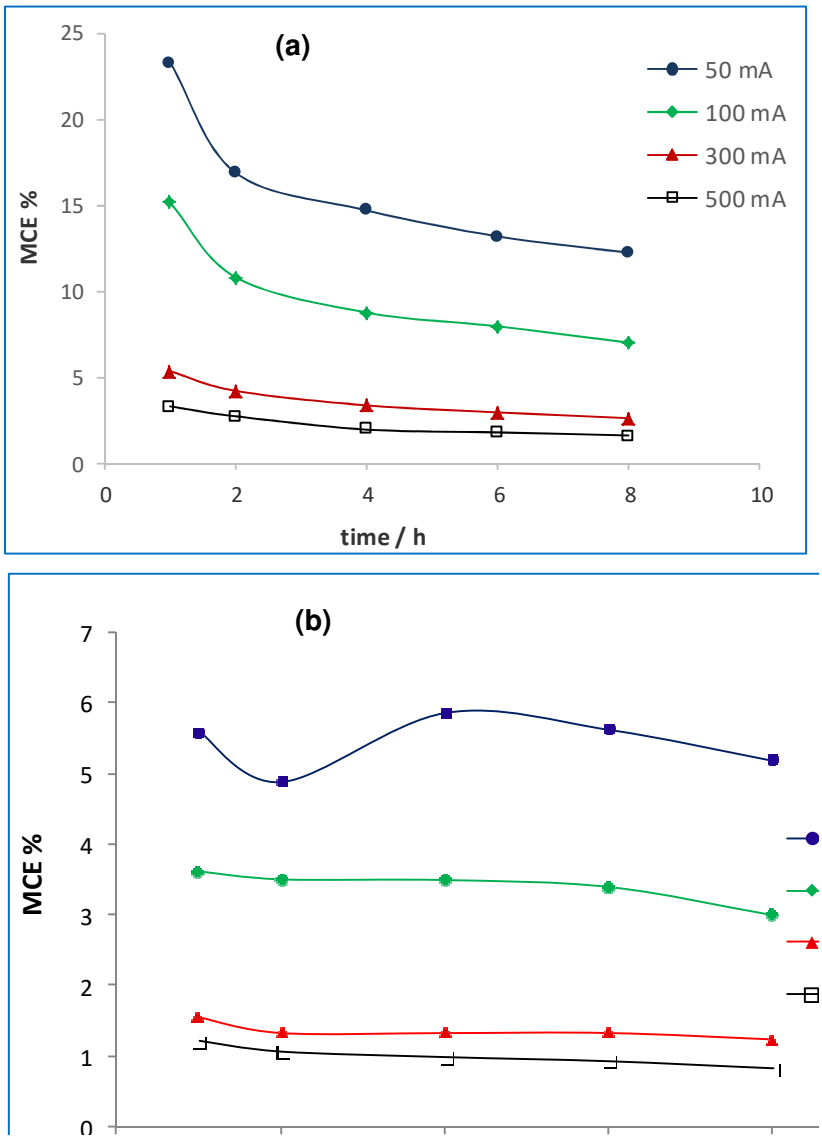

Figure 8